

## EDGE ARTICLE

[View Article Online](#)  
[View Journal](#) | [View Issue](#)



CrossMark  
click for updates

Cite this: *Chem. Sci.*, 2016, 7, 4364

# Visible-light-driven CO<sub>2</sub> reduction on a hybrid photocatalyst consisting of a Ru(II) binuclear complex and a Ag-loaded TaON in aqueous solutions†

Akinobu Nakada, Takuya Nakashima, Keita Sekizawa, Kazuhiko Maeda and Osamu Ishitani\*

A hybrid photocatalyst consisting of a Ru(II) binuclear complex and a Ag-loaded TaON reduced CO<sub>2</sub> by visible light even in aqueous solution. The distribution of the reduction products was strongly affected by the pH of the reaction solution. HCOOH was selectively produced in neutral conditions, whereas the formation of HCOOH competed with H<sub>2</sub> evolution in acidic conditions. Detailed mechanistic studies revealed that the photocatalytic CO<sub>2</sub> reduction proceeded via 'Z-schematic' electron transfer with step-by-step photoexcitation of TaON and the photosensitizer unit in the Ru(II) binuclear complex. The maximum turnover number for HCOOH formation was 750 based on the Ru(II) binuclear complex under visible-light irradiation, and the optimum external quantum efficiency of the HCOOH formation was 0.48% using 400 nm monochromatic light with ethylenediaminetetraacetic acid disodium salt as a sacrificial reductant. Even in aqueous solution, the hybrid could also convert visible-light energy into chemical energy ( $\Delta G^0 = +83 \text{ kJ mol}^{-1}$ ) by the reduction of CO<sub>2</sub> to HCOOH with methanol oxidation.

Received 6th February 2016  
Accepted 23rd March 2016

DOI: 10.1039/c6sc00586a  
[www.rsc.org/chemicalscience](http://www.rsc.org/chemicalscience)

## Introduction

The development of photocatalytic systems for CO<sub>2</sub> reduction is an attractive research target in the field of conversion of solar energy into chemical energy, the so-called artificial photosynthesis. Artificial photosynthetic reactions have various potential functions; one of these is to use water as both an electron source and as a solvent because water is an abundant and low-cost material. Since both CO<sub>2</sub> and water are very stable compounds, these photocatalytic systems should have both strong reduction and oxidation power. Utilization of visible light is another important function for artificial photosynthesis because it covers *ca.* 50% of the solar energy, whereas the light in the UV region ( $\lambda < 400 \text{ nm}$ ) is very minor (<6%). However, there are few visible-light-driven photocatalysts for CO<sub>2</sub> reduction which function well in water.

Multinuclear Ru(II) and/or Re(I) diimine (N<sup>+</sup>N) complexes with a redox photosensitizer (PS) and a catalyst (CAT) unit, the so-called supramolecular photocatalysts, have attractive abilities as photocatalysts for CO<sub>2</sub> reduction because of their high efficiencies and selectivities for reducing CO<sub>2</sub> to HCOOH and

CO not only in organic solution<sup>1–9</sup> but also in aqueous solution.<sup>10,11</sup> Since proton reduction to H<sub>2</sub> is a more thermodynamically favorable reaction than CO<sub>2</sub> reduction, this specific selectivity is a superior property for constructing an artificial photosynthesis system with CO<sub>2</sub> reduction in aqueous solution. However, the photocatalytic systems constructed with only metal complexes generally require a strong reductant such as NADH model compounds<sup>2–5,9</sup> and benzimidazoline derivatives<sup>1,3,4,11</sup> because the excited metal complexes have relatively weak oxidizing power. To add the stronger photooxidizing power, the metal complex photocatalyst should be combined with another photocatalyst for the oxidation reaction.

Some powder semiconductor photocatalysts with much stronger oxidizing power have been reported, which can oxidize even water involving reduction of electron acceptors.<sup>12</sup> Metal oxynitrides are typical examples; they have sufficient positive valence band potential to oxidize weak reductants and relatively small band gaps to utilize visible light.<sup>13</sup>

Based on these investigations regarding the strong and weak points of different types of photocatalysts, we have developed novel hybrid photocatalytic systems where supramolecular photocatalysts connect with metal oxynitride photocatalysts to utilize both the outstanding features of high selectivity and efficiency for CO<sub>2</sub> photoreduction (supramolecular site) and strong photooxidizing power (semiconductor site). Visible-light irradiation to the hybrid photocatalysts consisting of a Ru(II)

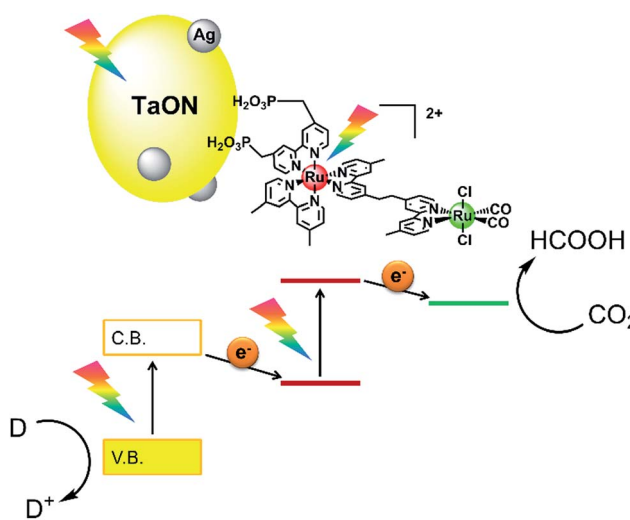
Department of Chemistry, Graduate School of Science and Engineering, Tokyo Institute of Technology, 2-12-1-NE-1 Ookayama, Meguro-ku, Tokyo 152-8550, Japan. E-mail: [ishitani@chem.titech.ac.jp](mailto:ishitani@chem.titech.ac.jp)

† Electronic supplementary information (ESI) available. See DOI: [10.1039/c6sc00586a](https://doi.org/10.1039/c6sc00586a)

binuclear complex (**RuRu**) with  $[\text{Ru}(\text{N}^{\wedge}\text{N})_3]^{2+}$  as the PS unit and  $\text{Ru}(\text{N}^{\wedge}\text{N})(\text{CO})_2\text{Cl}_2$  as the CAT unit, which was adsorbed on a tantalum(v) oxynitride (TaON) photocatalyst in pure methanol without any other reductant under a  $\text{CO}_2$  atmosphere, caused the catalytic formation of  $\text{HCOOH}$  as a reduced product of  $\text{CO}_2$  and formaldehyde as an oxidized product of methanol (MeOH).<sup>14</sup> Using  $\text{CaTaO}_2\text{N}$  instead of TaON in the hybrid achieved high selectivity of  $\text{HCOOH}$  formation (>99%) in dimethylacetamide-triethanolamine mixed solution; meanwhile, the photocatalytic reaction requires a sacrificial electron donor.<sup>15</sup> These reactions are driven *via* the two-step photoinduced electron transfer mechanism, the so-called 'Z-scheme', as shown in Scheme 1: (1) step-by-step photoexcitation of the semiconductor and the Ru(II) PS unit occurs; (2) the valence band holes are consumed by a reductant; (3) conduction band electrons in the semiconductor transfer to the excited state of the PS unit, producing one-electron-reduced species (OERS) of PS; (4) intramolecular electron transfer from the OERS of the PS unit to the ground state of the CAT unit occurs, producing the reduced CAT unit and (5)  $\text{CO}_2$  reduction proceeds on the reduced CAT.

Along with the Z-scheme hybrid photocatalysts, another powder hybrid photocatalyst consisting of a mononuclear metal complex as the CAT and a semiconductor such as carbon nitride<sup>16–18</sup> or nitrogen-doped  $\text{Ta}_2\text{O}_5$ <sup>19,20</sup> working as a PS have been developed for use in  $\text{CO}_2$  reduction.

However, these hybrid photocatalysts were investigated only in organic solutions; we do not have any information on their photocatalytic activity in water. In this work, the photocatalytic activity of the hybrid photocatalyst of Ag-modified TaON and the Ru(II) binuclear complex (**RuRu/Ag/TaON**, Scheme 1) was investigated for the first time in aqueous solutions containing electron donors, and we observed that **RuRu/Ag/TaON** photocatalyzed efficient  $\text{CO}_2$  reduction with high durability. This Z-schematic hybrid photocatalyst could also drive an uphill reaction, *i.e.*  $\text{CO}_2$  reduction with methanol as a reductant, in a water-methanol mixed solution.



Scheme 1 Hybrid powder photocatalyst of the Ru(II) binuclear complex adsorbed on Ag-modified TaON (RuRu/Ag/TaON).

## Results and discussion

A hybrid photocatalyst of Ag-modified TaON and a Ru(II) binuclear complex **RuRu/Ag/TaON** was synthesized according to a reported method.<sup>14</sup> Typically, the loaded amount of silver and **RuRu** were 1.5 wt% and 3  $\mu\text{mol g}^{-1}$ , respectively, except for the experiment corresponding to Fig. 5. The obtained materials were characterized by diffuse reflectance spectroscopy (DRS), X-ray diffraction (XRD), emission spectroscopy and Fourier-transform infrared (FT-IR) spectroscopy, as shown in Fig. 1 and S1–S3, ESI.† The XRD patterns of TaON, Ag/TaON and **RuRu/Ag/TaON** confirm that the crystal structure of TaON was not changed during the attachment procedures of silver and **RuRu** on TaON (Fig. S1a, ESI†). The typical diffraction peak at  $2\theta = 38.1^\circ$  is attributed to metallic silver; this peak appears in the spectra of Ag/TaON and **RuRu/Ag/TaON** (Fig. S1b, ESI†). Fig. 1 shows DRS spectra of the hybrids **RuRu/Ag/TaON**, Ag/TaON and TaON along with **RuRu/Al<sub>2</sub>O<sub>3</sub>**, which is a model of **RuRu**. A broad absorption band was observed in the cases of Ag/TaON and **RuRu/Ag/TaON**, which is due to surface plasmon resonance of the metallic silver particles on the surface of TaON. **RuRu/Ag/TaON** also exhibited an absorption attributable to the Ru(II) photosensitizer unit (Fig. 1 and S4, ESI†). A dispersion of **RuRu/Ag/TaON** in water showed emission with  $\lambda_{\text{em}} = 629$  nm by photoexcitation at  $\lambda_{\text{ex}} = 444$  nm, which is attributable to phosphorescence from the triplet metal-to-ligand charge transfer (<sup>3</sup>MLCT) excited state of the Ru(II) PS unit as well as phosphorescence from **RuRu** dissolved in water (Fig. S2, ESI†). IR absorption bands corresponding to the CO stretching vibrations of the Ru(II) CAT unit were observed at 2061 and 1997  $\text{cm}^{-1}$  in the FT-IR spectrum of **RuRu/Ag/TaON** (Fig. S3, ESI†). These spectroscopic results indicate that the structure of **RuRu** was maintained after adsorption on Ag/TaON.

As a typical run, a powder of **RuRu/Ag/TaON** (4 mg) was dispersed in aqueous solution (4 mL) containing ethylenediaminetetraacetic acid disodium salt (EDTA·2Na, 10 mM) and irradiated at  $\lambda_{\text{ex}} > 400$  nm under a  $\text{CO}_2$  atmosphere. After 24 h irradiation, formic acid,  $\text{H}_2$  and a small amount of CO were produced with turnover numbers (TON) of 750 (8.5  $\mu\text{mol}$ ), 1240

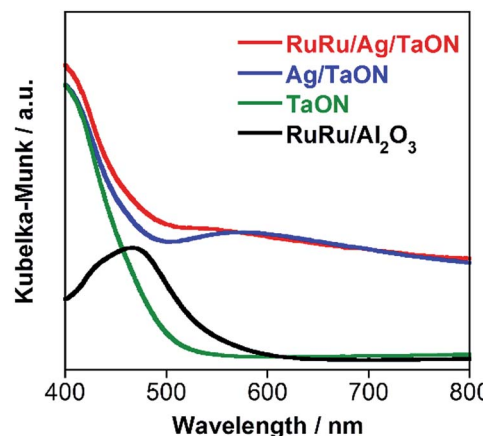


Fig. 1 DRS of **RuRu/Ag/TaON** (red), Ag/TaON (blue), TaON (green) and **RuRu/Al<sub>2</sub>O<sub>3</sub>** (black).



(14.2  $\mu\text{mol}$ ) and 30 (0.3  $\mu\text{mol}$ ), respectively (Fig. 2a). The external quantum yields ( $\Phi$ ) of the photocatalytic reaction were  $\Phi_{\text{HCOOH}} = 0.47\%$  and  $\Phi_{\text{H}_2} = 0.54\%$  using 400 nm monochromatic light. In contrast, formic acid was produced with much higher selectivity (85%) by addition of  $\text{Na}_2\text{CO}_3$  (0.1 M) to the reaction solution (Fig. 2b), although TON<sub>HCOOH</sub> (620) and  $\Phi_{\text{HCOOH}}$  (0.23%) were lower than those in the absence of  $\text{Na}_2\text{CO}_3$ . Details of this difference are described in a later part of this paper.

The carbon source of HCOOH was confirmed by an isotope-labeling experiment. A red line in Fig. 3 shows the  $^1\text{H}$  NMR spectrum of the reaction solution after the photocatalytic reaction under the same condition as that described above, except using  $^{13}\text{CO}_2$  instead of ordinary  $\text{CO}_2$ . A doublet attributed to  $\text{H}^{13}\text{COOH}$  was mainly observed at 8.31 ppm ( $^1J_{\text{CH}} = 196$  Hz), with a small singlet attributed to  $\text{H}^{12}\text{COOH}$ . In contrast, only a singlet of  $\text{H}^{12}\text{COOH}$  was observed for the photocatalysis under ordinary  $\text{CO}_2$  atmosphere (a blue line in Fig. 3). Based on the areas of these peaks, we calculated that 97% of HCOOH was formed by reduction of  $\text{CO}_2$  in the photocatalytic reaction. Notably, this value is comparable with the purity of the  $^{13}\text{CO}_2$  used (99%).

Table 1 summarizes the results of the photocatalytic reactions using various hybrids in aqueous solution containing EDTA·2Na (10 mM). Irradiation to **RuRu/Ag/Al<sub>2</sub>O<sub>3</sub>**, where Al<sub>2</sub>O<sub>3</sub> was used as an insulator instead of TaON, did not yield any reduction products (entry 2, Table 1). The oxidizing power of the excited photosensitizer unit in **RuRu** was evaluated by emission measurements using EDTA·2Na as a quencher (Fig. S5, ESI<sup>†</sup>). Only 7% of the emission from the  $^3\text{MLCT}$  excited state of the PS unit of **RuRu** on the surface of Al<sub>2</sub>O<sub>3</sub> was quenched by 10 mM of EDTA·2Na. These results suggest that EDTA·2Na mainly supplies electrons to the Ag/TaON unit in the photocatalytic reaction using **RuRu/Ag/TaON**. After the photocatalytic reaction using **RuRu/Ag/TaON**, we could not observe N<sub>2</sub> generation by gas chromatography. Furthermore, there were no differences in either the binding energy for the Ta4p peak or the ratio of areas for Ta4p and N1s of TaON in **RuRu/Ag/TaON** before and after the photocatalytic reaction by X-ray photoelectron spectroscopy (XPS) analysis (Fig. S6, ESI<sup>†</sup>). These observations indicate that the TaON unit in **RuRu/Ag/TaON** did not decompose during the photocatalytic reaction, which occasionally becomes a problem in some photocatalytic systems because it consumes

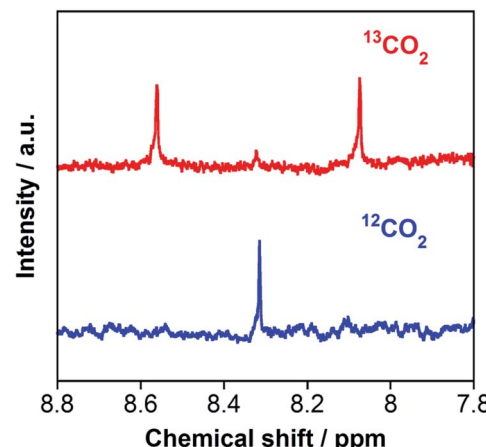


Fig. 3  $^1\text{H}$  NMR spectra of the aqueous reaction solutions (1 mL) containing **RuRu/Ag/TaON** (4 mg) and EDTA·2Na (10 mM), measured after 24 h irradiation at  $\lambda_{\text{ex}} > 400$  nm under  $^{13}\text{CO}_2$  (red) and  $^{12}\text{CO}_2$  (blue) atmospheres.

photo-generated holes by the decomposition of TaON itself (eqn (1)).<sup>21–25</sup>



Silver particles have been reported to act as a co-catalyst for  $\text{CO}_2$  reduction on some semiconductor photocatalysts which require irradiation of UV light.<sup>26–34</sup> However, Ag/TaON without **RuRu** did not photocatalyze  $\text{CO}_2$  reduction at all (entry 3 in Table 1), indicating that the silver particles of **RuRu/Ag/TaON** did not work as a co-catalyst for  $\text{CO}_2$  reduction. However, loading silver to the surface of TaON dramatically enhanced the photocatalytic activity of **RuRu/Ag/TaON**, particularly for  $\text{CO}_2$  reduction (compare entries 1 and 4, Table 1). It has been reported that loading of Ag on the surface of a hybrid photocatalyst **RuRu/CaTaO<sub>2</sub>N** enhances the photoinduced electron transfer from the conduction band of CaTaO<sub>2</sub>N to the excited states of the Ru photosensitizer unit.<sup>15</sup> A similar phenomenon

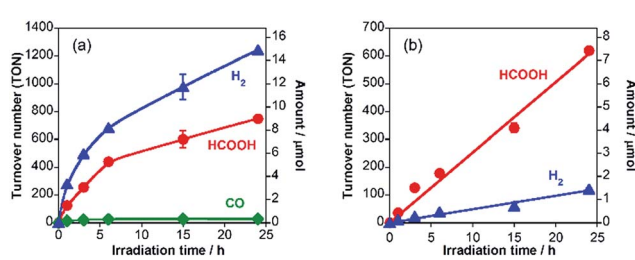


Fig. 2 Time courses of HCOOH (red),  $\text{H}_2$  (blue) and CO (green) formation by visible-light ( $\lambda > 400$  nm) irradiation to **RuRu/Ag/TaON** (4 mg) in EDTA·2Na (10 mM) aqueous solution (4 mL) without (a) and with (b)  $\text{Na}_2\text{CO}_3$  (0.1 M) under a  $\text{CO}_2$  atmosphere.

Table 1 Photocatalytic reactions using various hybrids under a  $\text{CO}_2$  atmosphere<sup>a</sup>

Entry	Photocatalyst	Product/ $\mu\text{mol}$ (TON)		
		HCOOH	CO	$\text{H}_2$
1	<b>RuRu/Ag/TaON</b>	7.0 (600)	0.3 (28)	11.4 (978)
2	<b>RuRu/Ag/Al<sub>2</sub>O<sub>3</sub></b>	N.D.	N.D.	N.D.
3	Ag/TaON	N.D.	N.D.	0.4 (–)
4	<b>RuRu/TaON</b>	1.2 (103)	0.2 (16)	5.0 (420)
5	<b>Ru(Cat)<sup>b</sup>/Ag/TaON</b>	<0.1 (–)	N.D.	<0.1 (–)
6	<b>Ru(PS)<sup>c</sup>/Ag/TaON</b>	<0.1 (–)	N.D.	4.2 (371)

<sup>a</sup> Dispersion of a photocatalyst (4 mg) in an EDTA·2Na (10 mM) aqueous solution (4 mL) was irradiated at  $\lambda_{\text{ex}} > 400$  nm for 15 h. <sup>b</sup> **Ru(Cat)** = *cis*-Ru{4,4'-(CH<sub>2</sub>PO<sub>3</sub>H<sub>2</sub>)<sub>2</sub>-2,2'-bipyridine}(CO)<sub>2</sub>Cl<sub>2</sub>. <sup>c</sup> **Ru(PS)** = [Ru(dmb)<sub>2</sub>{4,4'-(CH<sub>2</sub>PO<sub>3</sub>H<sub>2</sub>)<sub>2</sub>-2,2'-bipyridine}](PF<sub>6</sub>)<sub>2</sub>.



should accelerate the photocatalytic ability of **RuRu**/Ag/TaON in the present system.

Use of the mononuclear model complex of the CAT unit (**Ru(Cat)**) instead of **RuRu** drastically lowered the photocatalytic activity of the hybrid (entry 5, Table 1). This is reasonable because the electron transfer from the conduction band of TaON ( $E_{CBM} = -1.31$  V)<sup>14</sup> to **Ru(Cat)** ( $E_p^{\text{red}} = -1.46$  V vs. Ag/AgCl at pH 7)<sup>14</sup> is an endergonic reaction. A hybrid without the catalyst unit (**Ru(PS)**/Ag/TaON), *i.e.* a mononuclear model complex of the PS unit (**Ru(PS)**) adsorbed on Ag/TaON, produced a catalytic amount of H<sub>2</sub> with a very small amount of HCOOH (entry 6, Table 1). There have been some reports that [Ru(N<sup>+</sup>N)<sub>3</sub>]<sup>2+</sup>-type complexes decompose *via* photoinduced-ligand-substitution reactions to produce [Ru(N<sup>+</sup>N)<sub>2</sub>(X)(Y)]<sup>n+</sup>-type complexes,<sup>35,36</sup> and the product [Ru(N<sup>+</sup>N)<sub>2</sub>(X)(Y)]<sup>n+</sup> acts as a catalyst for both H<sub>2</sub> evolution and CO<sub>2</sub> reduction with the residual [Ru(N<sup>+</sup>N)<sub>3</sub>]<sup>2+</sup> as the photosensitizer.<sup>10,11,37</sup> From these control experiments and the emission quenching measurements, we can conclude that all of the units in the hybrid photocatalyst **RuRu**/Ag/TaON are necessary for the efficient photocatalytic reduction of CO<sub>2</sub>. **RuRu**/Ag/TaON worked *via* the Z-schematic electron-transfer mechanism from EDTA·2Na to the Ru catalyst unit with visible-light photoexcitation of both TaON and the Ru photosensitizer unit with the assistance of the Ag particles on the surface of TaON, followed by the CO<sub>2</sub> reduction proceeding on the Ru catalyst unit, as shown in Scheme 1.

The effects of coexistent ions and the pH of the reaction solution on the photocatalytic activity were examined in detail with a series of additional salts to the reaction solution. Table 2 summarizes the results using EDTA·2Na (10 mM) as an electron donor, including the produced amounts of the reduction products, the selectivity of CO<sub>2</sub> reduction ( $\text{sel}_{\text{CO}_2}$ ) and the desorption ratios of the surface-bound **RuRu** ( $\eta_{\text{des}}$ ). Addition of Na<sub>2</sub>CO<sub>3</sub> (entry 2 in Table 2), K<sub>2</sub>CO<sub>3</sub> (entry 3) and Na<sub>2</sub>HPO<sub>4</sub> (entry 4), which changed the pH of the reaction solution to between

6.5 and 7.0, dramatically improved the selectivity of CO<sub>2</sub> reduction. On the other hand, the change in ion strength of the reaction solution should not be a reason for this change in selectivity because the selectivity did not change in reaction solutions containing various concentrations of Na<sub>2</sub>HPO<sub>4</sub> (34–35%, pH = 4.4, entries 5–7), where the pH was similar to that without the salts (37%, pH = 4.3, entry 1). Fig. 4a (plots of entries 1–8 and 11) exhibit clear trend that higher pH increased the selectivity of CO<sub>2</sub> reduction unrelated to the ion strength of the solution; a more basic solution suppresses the evolution of H<sub>2</sub>, probably because of the lower proton concentration in the reaction solution.

The produced amounts of HCOOH were lowered by the addition of the salts (0.1 M), regardless of the solution pH (entries 2–5). The UV-vis absorption spectra of the filtrates of the reaction solutions after the photocatalytic reactions exhibit an absorption band attributed to **RuRu** (Fig. S7, ESI†), indicating that **RuRu** partially desorbed from **RuRu**/Ag/Al<sub>2</sub>O<sub>3</sub> during the photocatalytic reaction. Ru(II) diimine complexes with phosphonic acid anchor groups have been widely used as a photosensitizer in various photocatalytic systems<sup>14–19,38–41</sup> and dye-sensitized photoelectrochemical cells.<sup>42–50</sup> It was reported that in many cases, desorption of Ru complexes from the surface of metal oxides proceeded under visible-light irradiation in aqueous solution.<sup>51–54</sup> The  $\eta_{\text{des},S}$  were 52–60% in the presence of the salts (0.1 M; entries 2–5), which were three times larger than those in the absence of the salts (entry 1). Higher concentration of salts in the reaction solution induced higher  $\eta_{\text{des}}$  and lower TON (Fig. 4b), while lower concentration of salts suppressed the desorption of the metal complex and deactivation of the photocatalytic reaction (entries 1 and 6–8 in Table 2 and Fig. 4b). On the other hand, the pH of the solution and the type of added salts did not strongly affect  $\eta_{\text{des}}$  (entries 2–5). A mixed system of Ag/TaON (4 mg) and a Ru(II) binuclear complex without the methyl phosphonate anchoring groups (12 nmol) showed much lower photocatalytic abilities (compare entry 1

**Table 2** Results of photocatalytic reactions using **RuRu**/Ag/TaON (4 mg) in EDTA·2Na (10 mM) aqueous solutions containing various salts (4 mL) under visible-light ( $\lambda > 400$  nm) irradiation for 15 h

Entry	Salt <sup>a</sup>	pH <sup>b</sup>	Product/μmol (TON)				$\text{sel}_{\text{CO}_2}^c/\%$	$\eta_{\text{des}}/\%$
			HCOOH	CO	H <sub>2</sub>			
1	None	4.3	7.0 (600)	0.3 (28)	11.4 (978)	37	17	
2	Na <sub>2</sub> CO <sub>3</sub>	7.0	4.0 (340)	N.D.	0.7 (60)	85	58	
3	K <sub>2</sub> CO <sub>3</sub>	7.0	3.7 (307)	N.D.	0.9 (74)	81	60	
4	Na <sub>2</sub> HPO <sub>4</sub>	6.5	5.6 (482)	<0.1	2.0 (172)	74	58	
5	NaH <sub>2</sub> PO <sub>4</sub>	4.4	3.2 (257)	<0.1	6.1 (481)	35	52	
6	NaH <sub>2</sub> PO <sub>4</sub> <sup>d</sup>	4.4	3.9 (327)	<0.1	7.9 (658)	34	37	
7	NaH <sub>2</sub> PO <sub>4</sub> <sup>e</sup>	4.4	4.8 (421)	0.2 (13)	9.0 (791)	34	32	
8	Na <sub>2</sub> HPO <sub>4</sub> <sup>f</sup> + NaH <sub>2</sub> PO <sub>4</sub> <sup>f</sup>	6.1	4.8 (418)	<0.1	2.8 (245)	63	53	
9 <sup>g</sup>	None	4.3	0.7 (56)	N.D.	0.5 (46)	32	—	
10 <sup>h</sup>	None	4.3	1.3 (350)	<0.1	2.9 (773)	55	—	
11 <sup>i</sup>	None	5.9	6.7 (589)	0.1 (12)	4.8 (418)	58	26	

<sup>a</sup> Concentration was 0.1 M except for entries 6–8. <sup>b</sup> After purging with CO<sub>2</sub> for 20 min. <sup>c</sup> Selectivity of CO<sub>2</sub> reduction. <sup>d</sup> Concentration was 0.03 M.

<sup>e</sup> Concentration was 0.01 M. <sup>f</sup> Concentration was 0.05 M. <sup>g</sup> Using Ag/TaON (4 mg) and Ru(bpy)<sub>2</sub>(CH<sub>3</sub>bpyCH<sub>2</sub>CH<sub>2</sub>bpyCH<sub>3</sub>)Ru(CO)<sub>2</sub>Cl<sub>2</sub> (12 nmol).

<sup>h</sup> Adsorption amount of **RuRu** was 1.0 μmol g<sup>-1</sup>. <sup>i</sup> Using ethylenediaminetetraacetic acid tetrasodium salt (EDTA·4Na, 10 mM) instead of EDTA·2Na.



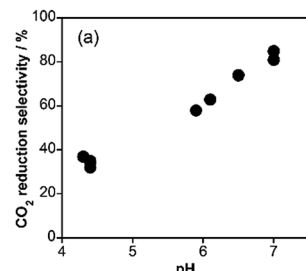


Fig. 4 (a) Selectivity of CO<sub>2</sub> reduction ( $\text{sel}_{\text{CO}_2}$ ) vs. pH of the reaction solution in the photocatalytic reactions. (b) Produced amount of HCOOH vs. desorption ratio of RuRu ( $\eta_{\text{des}}$ ) by the photocatalytic reactions with various concentration of NaH<sub>2</sub>PO<sub>4</sub> (pH = 4.4).

and entry 9). Therefore, the addition of salts accelerated the desorption of **RuRu**, lowering the photocatalytic activity of **RuRu/Ag/TaON**. This is also supported by the following experimental data: the use of **RuRu/Ag/TaON** with a smaller amount of **RuRu** (1.0 μmol g<sup>-1</sup>) produced much smaller amounts of HCOOH and H<sub>2</sub> (1.3 and 2.9 μmol, entry 10) compared with **RuRu/Ag/TaON** with 3.0 μmol g<sup>-1</sup> of **RuRu** (7.0 μmol of HCOOH and 11.4 μmol of H<sub>2</sub>, entry 1). The details of the effects of the adsorbed amount of **RuRu** on the activity are described later. Taking into account these effects of pH and concentration of additives, higher selective HCOOH formation (58% selectivity) was obtained when ethylenediaminetetraacetic acid tetrasodium salt (EDTA·4Na, pH = 5.9; entry 11) was used instead of EDTA·2Na (pH = 4.3; entry 1) keeping high TON of 589 for HCOOH formation.

Fig. 5 shows the external quantum efficiencies for photocatalytic HCOOH production ( $\Phi_{\text{HCOOH}}$ ) using **RuRu/Ag/TaON** with various loading amounts of **RuRu**. The  $\Phi_{\text{HCOOH}}$  increased with increasing loading amount of **RuRu** from 1.0 to 3.0 μmol g<sup>-1</sup> and then reached plateau with the maximum values of  $\Phi_{\text{HCOOH}} = 0.48\%$  at 8.3 μmol g<sup>-1</sup>. This is probably why the separation of the electron–hole pairs in TaON was accelerated

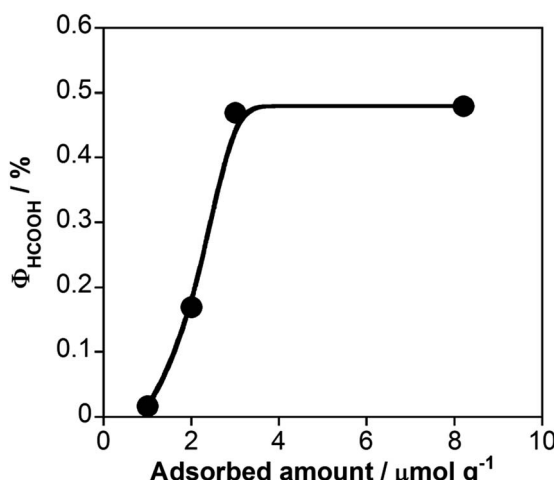


Fig. 5 Relationship between  $\Phi_{\text{HCOOH}}$  and loading amount of **RuRu** in the photocatalytic reaction using **RuRu/Ag/TaON** (30 mg) and EDTA·2Na (10 mM) in aqueous solution (10 mL) with 400 nm monochromatic light irradiation under a CO<sub>2</sub> atmosphere.

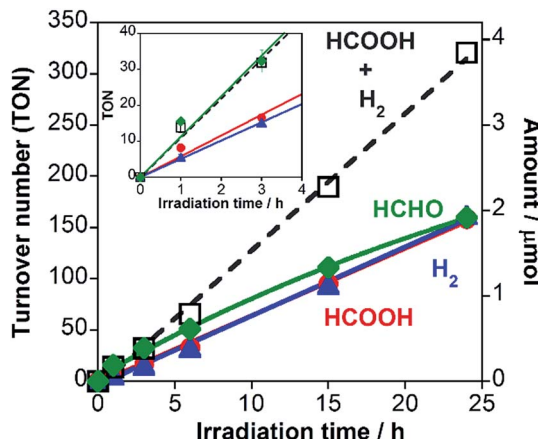


Fig. 6 Time courses of HCOOH (red), H<sub>2</sub> (blue) and HCHO (green) formation along with the sum of HCOOH and H<sub>2</sub> (black broken line) in the photocatalytic reaction: **RuRu/Ag/TaON** (4 mg) in a H<sub>2</sub>O–MeOH (4 : 1 v/v) mixed solution (4 mL) was irradiated by visible light ( $\lambda > 400$  nm) under a CO<sub>2</sub> atmosphere. Inset shows enlarged time courses until 4 h irradiation.

because of the electron transfer from the conduction band to **RuRu**. The loading amount of 3.0 μmol g<sup>-1</sup> might be sufficient to produce this effect. Notably,  $\Phi_{\text{HCOOH}}$  is the highest value obtained for photocatalytic CO<sub>2</sub> reduction using semiconductor–photosensitizer–catalyst triad systems to date.

We have already reported that **RuRu/Ag/TaON** can use methanol as a reductant for CO<sub>2</sub> reduction in pure methanol.<sup>14</sup> This is important because CO<sub>2</sub> reduction with methanol oxidation producing HCOOH as a reduced product of CO<sub>2</sub> and HCHO as an oxidized product of methanol (eqn (2)) is an endergonic reaction ( $\Delta G^0 = +83$  kJ mol<sup>-1</sup>); in other words, the visible-light energy is converted into chemical energy *via* the photocatalytic CO<sub>2</sub> reduction reaction. As the next step, in this study, we investigated whether the same endergonic CO<sub>2</sub> conversion reaction can proceed even in aqueous solution. Fig. 6 shows a time course of the TONs of both reduction products (HCOOH and H<sub>2</sub>) and an oxidation product (formaldehyde) in a photocatalytic reaction using **RuRu/Ag/TaON** in a H<sub>2</sub>O–MeOH mixed solution (4 : 1 v/v) without any other reductants. HCOOH and H<sub>2</sub> were produced continuously and TON<sub>HCOOH</sub> reached 17 at 3 h of irradiation. Formaldehyde was also formed, whose produced amount corresponded to the total of HCOOH and H<sub>2</sub> (Fig. 6 inset). This indicates that the overall reaction of the CO<sub>2</sub> reduction can be represented in eqn (2).



However, further irradiation induced less production of formaldehyde than the sum of HCOOH and H<sub>2</sub> (Fig. 6). We employed a <sup>13</sup>CO<sub>2</sub> labelling experiment to clarify the carbon sources of HCOOH. Fig. 7a shows the <sup>1</sup>H NMR spectrum of the filtered reaction solution after irradiation for 48 h; a doublet signal with  $J_{\text{CH}} = 204$  Hz and a singlet at 8.21 ppm are attributed to the methine protons of H<sup>13</sup>COOH and H<sup>12</sup>COOH, respectively. From this spectrum, we estimated that the main



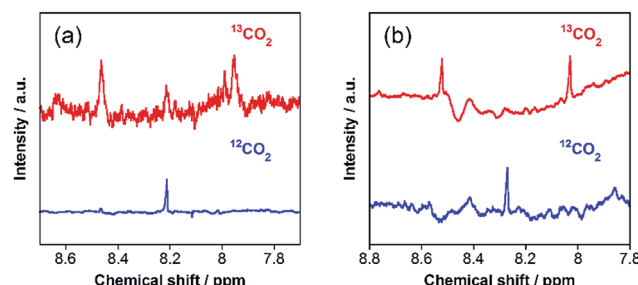


Fig. 7  $^1\text{H}$  NMR spectra of reaction solutions (2 mL) containing **RuRu**/Ag/TaON (8 mg) in (a)  $\text{H}_2\text{O}$ –MeOH (4 : 1 v/v) and (b)  $\text{H}_2\text{O}$ –iPrOH (4 : 1 v/v) after a 48 h irradiation with visible light ( $\lambda > 400$  nm) under  $^{13}\text{CO}_2$  (red) and  $^{12}\text{CO}_2$  (blue) atmospheres.

carbon source of  $\text{HCOOH}$  was  $\text{CO}_2$  (86%), although there were other carbon sources (14%). To gather information on the other carbon sources, a similar photocatalytic reaction was conducted using 2-propanol (i-PrOH) instead of methanol. This photocatalytic system also yielded  $\text{HCOOH}$  with  $\text{TON}_{\text{HCOOH}} = 58$  after 15 h of irradiation but did not give any  $\text{HCHO}$ . Fig. 7b shows the result of a  $^{13}\text{CO}_2$  labelling experiment using i-PrOH as the reductant; the  $^1\text{H}$  NMR spectrum of the filtered reaction solution after 48 h irradiation exhibits that the  $\text{HCOOH}$  was completely produced from  $\text{CO}_2$ . Therefore, when methanol was used as the reductant, partial  $\text{HCOOH}$  produced in the photocatalytic reduction was probably generated by further oxidation of  $\text{HCHO}$ , which was produced by oxidation of the methanol. This is also supported by the following result: the photocatalytic oxidation of MeOH using TaON as a photocatalyst and  $\text{AgNO}_3$  as a sacrificial oxidant in aqueous solution containing MeOH yielded not only  $\text{HCHO}$  as a main product but also  $\text{HCOOH}$  as a minor one (Fig. S8, ESI $^\dagger$ ). This minor formation process of  $\text{HCOOH}$  should contribute to determining the product distribution after a certain amount of  $\text{HCHO}$  was generated in the reaction solution. As described above, the ‘mismatch’ between the amount of  $\text{HCHO}$  and the total amount of  $\text{HCOOH}$  and  $\text{H}_2$  was initially observed after a 6 h irradiation, and a longer irradiation increased this mismatch.

## Experiments

### General procedures

UV-vis absorption spectra were measured with a JASCO V-565 spectrophotometer. X-ray diffraction was measured with a Rigaku MiniFlex 600. FT-IR spectra were measured at  $1\text{ cm}^{-1}$  resolution with a JASCO FT/IR-610 spectrophotometer. Emission spectra were measured at  $298 \pm 0.1\text{ K}$  with a JASCO FP-6500 spectrofluorometer. Emission lifetimes were measured with a Horiba FluoroCube 1000U-S time-correlated single-photon-counting system (the excitation source was a nano-LED 440L, and the instrument response was less than 1 ns).

### Materials

**RuRu**/Ag/TaON was synthesized according to a literature procedure. $^{14}$  Briefly, an  $\text{AgNO}_3$  (137  $\mu\text{M}$ ) aqueous solution

(10 mL) was added dropwise to a dispersion (100 mg) of TaON in water (10 mL), followed by stirring for 2 h. Then the suspension was evaporated and the residue was heated at 473 K for 1 h under a  $\text{H}_2$  atmosphere to obtain 1.5 wt% Ag-modified TaON (Ag/TaON). Then, a moderate amount of Ag/TaON was soaked in an acetonitrile solution of the Ru(II) binuclear complex (**RuRu**) for 3 h to obtain **RuRu**/Ag/TaON. The adsorption amount was estimated by the UV-vis absorbance changes of the solution before and after soaking (Fig. S4, ESI $^\dagger$  shows an example of a **RuRu** adsorbed sample with a loading amount of 3  $\mu\text{mol g}^{-1}$ ).

$\text{Ag}/\text{Al}_2\text{O}_3$  and  $\text{Ag}/\text{TiO}_2$  were prepared by the same impregnation–hydrogenation method followed by adsorption of **RuRu** as **RuRu**/Ag/TaON for  $\text{Al}_2\text{O}_3$  (AEROXIDE Alu C, AEROSIL) and  $\text{TiO}_2$  (AEROXIDE TiO<sub>2</sub> P25, AEROSIL), respectively.

Tap water was purified using a Millipore Elix Essential 3 UV system and used on the same day. Methanol was used after distillation. Absolute 2-propanol was purchased from Kanto Chemical Co., Inc. and used without purification. Other materials were reagent-grade quality and were used without further purification.

### Photocatalytic reactions

A suspension of photocatalyst (4 mg) in a reaction solution (4 mL) was prepared in an 8 mL test tube (i.d. = 8 mm) and purged with  $\text{CO}_2$ . The suspensions were irradiated by stirring using a photocatalytic reactor (Koike Precision Instruments) at  $\lambda > 400$  nm with a high-pressure Hg lamp combined with a  $\text{NaNO}_2$  aqueous solution filter. The temperatures of the solutions were controlled at  $298 \pm 2\text{ K}$  using an EYELA constant temperature system (CTP-1000) during irradiation. The quantum yield for  $\text{HCOOH}$  and  $\text{H}_2$  formation was evaluated in a reaction cell containing **RuRu**/Ag/TaON (30 mg) in a reaction solution (10 mL), which was irradiated with 400 nm monochromatic light using a 300 W Xe-lamp (Asahi Spectrum MAX-303) with a band pass filter (fwhm = 10 nm). The gaseous reaction products, *i.e.*  $\text{CO}$  and  $\text{H}_2$ , were analyzed by a GC-TCD (GL Science GC 323).  $\text{HCOOH}$  in the liquid phase was analyzed by a capillary electrophoresis system (Otsuka Electronics Co. Capi-3300I).  $\text{HCHO}$  was quantitated by a colorimetric analysis following a reported procedure. $^{14}$

We evaluated the photocatalytic activity of the hybrids by using turnover number (TON, eqn (3)), selectivity (eqn (4)) and external quantum efficiency ( $\Phi$ , eqn (5)).

$$\text{TON} = \frac{\text{product(mol)}}{\text{RuRu used(mol)}} \quad (3)$$

$$\text{Selectivity} = \frac{\text{CO}_2 \text{ reduction product(mol)}}{\text{reduction products(mol)}} \quad (4)$$

$$\Phi = \frac{\text{product(mol)}}{\text{imputed photon(einstein)}} \quad (5)$$

### $^{13}\text{CO}_2$ labelling experiments

$^{13}\text{CO}_2$  labelling experiments in  $\text{EDTA} \cdot 2\text{Na}$  (10 mM) aqueous solution were performed using a dispersion of **RuRu**/Ag/TaON (4 mg) in aqueous solution (1 mL) containing  $\text{EDTA} \cdot 2\text{Na}$



(10 mM) in a reaction cell. The cell was degassed using the freeze–pump–thaw method, and then  $^{13}\text{CO}_2$  (99%, 703 mmHg) was introduced into it. For the photocatalytic system in  $\text{H}_2\text{O}$ –MeOH mixed solution, a suspension of RuRu/Ag/TaON (8 mg) in a  $\text{H}_2\text{O}$ –MeOH (2 mL, 4 : 1 v/v) mixed solution in an 8 mL test tube was purged with  $^{13}\text{CO}_2$  (99%) for 20 min. The suspensions were irradiated using a photocatalytic reactor (Koike Precision Instruments) at  $\lambda > 400$  nm with a high-pressure Hg lump combined with a  $\text{NaNO}_2$  aqueous solution filter. After photolysis, the reaction solution was analyzed by  $^1\text{H}$  NMR by using a JEOL ECA400II (400 MHz) system with a No-D technique following filtration.

## Conclusions

A hybrid of a supramolecular photocatalyst with both Ru(II) photosensitizer and catalyst units, and Ag-loaded TaON photocatalyzed  $\text{CO}_2$  reduction, even in aqueous solution; step-by-step photoexcitation of the Ru(II) photosensitizer unit and TaON could induce both strong reducing and oxidizing power in the hybrid photocatalyst, and relatively efficient  $\text{CO}_2$  reduction giving  $\text{HCOOH}$  proceeded with high durability in aqueous solution containing  $\text{EDTA}\cdot 2\text{Na}$  as an electron donor. This Z-scheme-type hybrid photocatalyst could also induce reduction of  $\text{CO}_2$  with methanol as the reductant giving  $\text{HCOOH}$  and  $\text{HCHO}$  even in aqueous solution, where the visible-light energy was converted into chemical energy ( $\Delta G^0 = +83 \text{ kJ mol}^{-1}$ ).

## Acknowledgements

This work was supported by CREST/JST and a Grant-in-Aid for Scientific Research on Innovative Areas “Artificial photosynthesis (AnApple)” (No. 24107005) from the Japan Society for the Promotion of Science (JSPS). K. M. acknowledges the Noguchi Institute for financial support. The authors also thank AEROSIL for supplying  $\text{TiO}_2$  and  $\text{Al}_2\text{O}_3$  materials.

## References

- 1 Y. Tamaki, K. Koike and O. Ishitani, *Chem. Sci.*, 2015, **6**, 7213–7221.
- 2 E. Kato, H. Takeda, K. Koike, K. Ohkubo and O. Ishitani, *Chem. Sci.*, 2015, **6**, 3003–3012.
- 3 Y. Tamaki, K. Koike, T. Morimoto and O. Ishitani, *J. Catal.*, 2013, **304**, 22–28.
- 4 Y. Tamaki, K. Koike, T. Morimoto, Y. Yamazaki and O. Ishitani, *Inorg. Chem.*, 2013, **52**, 11902–11909.
- 5 Y. Tamaki, K. Watanabe, K. Koike, H. Inoue, T. Morimoto and O. Ishitani, *Faraday Discuss.*, 2012, **155**, 115–127.
- 6 Y. Tamaki, T. Morimoto, K. Koike and O. Ishitani, *Proc. Natl. Acad. Sci. U. S. A.*, 2012, **109**, 15673–15678.
- 7 K. Koike, S. Naito, S. Sato, Y. Tamaki and O. Ishitani, *J. Photochem. Photobiol. A*, 2009, **207**, 109–114.
- 8 S. Sato, K. Koike, H. Inoue and O. Ishitani, *Photochem. Photobiol. Sci.*, 2007, **6**, 454–461.
- 9 B. Gholamkhass, H. Mametsuka, K. Koike, T. Tanabe, M. Furue and O. Ishitani, *Inorg. Chem.*, 2005, **44**, 2326–2336.
- 10 A. Nakada, K. Koike, T. Nakashima, T. Morimoto and O. Ishitani, *Inorg. Chem.*, 2015, **54**, 1800–1807.
- 11 A. Nakada, K. Koike, K. Maeda and O. Ishitani, *Green Chem.*, 2016, **18**, 139–143.
- 12 A. Kudo and Y. Miseki, *Chem. Soc. Rev.*, 2009, **38**, 253–278.
- 13 K. Maeda, *Phys. Chem. Chem. Phys.*, 2013, **15**, 10537–10548.
- 14 K. Sekizawa, K. Maeda, K. Domen, K. Koike and O. Ishitani, *J. Am. Chem. Soc.*, 2013, **135**, 4596–4599.
- 15 F. Yoshitomi, K. Sekizawa, K. Maeda and O. Ishitani, *ACS Appl. Mater. Interfaces*, 2015, **7**, 13092–13097.
- 16 R. Kuriki, K. Sekizawa, O. Ishitani and K. Maeda, *Angew. Chem., Int. Ed.*, 2015, **54**, 2406–2409.
- 17 K. Maeda, R. Kuriki, M. Zhang, X. Wang and O. Ishitani, *J. Mater. Chem. A*, 2014, **2**, 15146–15151.
- 18 K. Maeda, K. Sekizawa and O. Ishitani, *Chem. Commun.*, 2013, **49**, 10127–10129.
- 19 T. M. Suzuki, H. Tanaka, T. Morikawa, M. Iwaki, S. Sato, S. Saeki, M. Inoue, T. Kajino and T. Motohiro, *Chem. Commun.*, 2011, **47**, 8673–8675.
- 20 S. Sato, T. Morikawa, S. Saeki, T. Kajino and T. Motohiro, *Angew. Chem., Int. Ed.*, 2010, **49**, 5101–5105.
- 21 G. Hitoki, T. Takata, J. N. Kondo, M. Hara, H. Kobayashi and K. Domen, *Chem. Commun.*, 2002, 1698–1699.
- 22 M. Hara, G. Hitoki, T. Takata, J. N. Kondo, H. Kobayashi and K. Domen, *Catal. Today*, 2003, **78**, 555–560.
- 23 M. Higashi, K. Domen and R. Abe, *Energy Environ. Sci.*, 2011, **4**, 4138–4147.
- 24 R. Abe, M. Higashi and K. Domen, *J. Am. Chem. Soc.*, 2010, **132**, 11828–11829.
- 25 K. Maeda, R. Abe and K. Domen, *J. Phys. Chem. C*, 2011, **115**, 3057–3064.
- 26 Z. Wang, K. Teramura, S. Hosokawa and T. Tanaka, *J. Mater. Chem. A*, 2015, **3**, 11313–11319.
- 27 K. Teramura, H. Tatsumi, Z. Wang, S. Hosokawa and T. Tanaka, *Bull. Chem. Soc. Jpn.*, 2015, **88**, 431–437.
- 28 Z. Wang, K. Teramura, S. Hosokawa and T. Tanaka, *Appl. Catal., B*, 2015, **163**, 241–247.
- 29 T. Takayama, K. Tanabe, K. Saito, A. Iwase and A. Kudo, *Phys. Chem. Chem. Phys.*, 2014, **16**, 24417–24422.
- 30 T. Takayama, A. Iwase and A. Kudo, *Bull. Chem. Soc. Jpn.*, 2015, **88**, 538–543.
- 31 K. Iizuka, T. Wato, Y. Miseki, K. Saito and A. Kudo, *J. Am. Chem. Soc.*, 2011, **133**, 20863–20868.
- 32 N. Yamamoto, T. Yoshida, S. Yagi, Z. Like, T. Mizutani, S. Ogawa, H. Nameki and H. Yoshida, *e-J. Surf. Sci. Nanotechnol.*, 2014, **12**, 263–268.
- 33 M. Yamamoto, T. Yoshida, N. Yamamoto, T. Nomoto, Y. Yamamoto, S. Yagi and H. Yoshida, *J. Mater. Chem. A*, 2015, **3**, 16810–16816.
- 34 M. Yamamoto, T. Yoshida, N. Yamamoto, T. Nomoto and S. Yagi, *Nucl. Instrum. Methods Phys. Res., Sect. B*, 2015, **359**, 64–68.
- 35 P. E. Hoggard and G. B. Porter, *J. Am. Chem. Soc.*, 1978, **100**, 1457–1463.
- 36 J. Van Houten and R. J. Watts, *Inorg. Chem.*, 1978, **17**, 3381–3385.



37 J.-M. Lehn and R. Ziessel, *J. Organomet. Chem.*, 1990, **382**, 157–173.

38 K. Maeda, M. Eguchi, S.-H. A. Lee, W. J. Youngblood, H. Hata and T. E. Mallouk, *J. Phys. Chem. C*, 2009, **113**, 7962–7969.

39 W. J. Youngblood, S.-H. A. Lee, K. Maeda and T. E. Mallouk, *Acc. Chem. Res.*, 2009, **42**, 1966–1973.

40 K. Maeda, G. Sahara, M. Eguchi and O. Ishitani, *ACS Catal.*, 2015, **5**, 1700–1707.

41 Y. Ueda, H. Takeda, T. Yui, K. Koike, Y. Goto, S. Inagaki and O. Ishitani, *ChemSusChem*, 2015, **8**, 439–442.

42 B. H. Farnum, A. Nakada, O. Ishitani and T. J. Meyer, *J. Phys. Chem. C*, 2015, **119**, 25180–25187.

43 G. Sahara, R. Abe, M. Higashi, T. Morikawa, K. Maeda, Y. Ueda and O. Ishitani, *Chem. Commun.*, 2015, **51**, 10722–10725.

44 B. D. Sherman, D. L. Ashford, A. M. Lapides, M. V. Sheridan, K.-R. Wee and T. J. Meyer, *J. Phys. Chem. Lett.*, 2015, **6**, 3213–3217.

45 A. M. Lapides, B. D. Sherman, M. K. Brennaman, C. J. Dares, K. R. Skinner, J. L. Templeton and T. J. Meyer, *Chem. Sci.*, 2015, **6**, 6398–6406.

46 M. V. Sheridan, B. D. Sherman, Z. Fang, K.-R. Wee, M. K. Coggins and T. J. Meyer, *ACS Catal.*, 2015, **5**, 4404–4409.

47 L. Alibabaei, B. D. Sherman, M. R. Norris, M. K. Brennaman and T. J. Meyer, *Proc. Natl. Acad. Sci. U. S. A.*, 2015, **112**, 5899–5902.

48 F. Li, K. Fan, L. Wang, Q. Daniel, L. Duan and L. Sun, *ACS Catal.*, 2015, **5**, 3786–3790.

49 X. Ding, Y. Gao, L. Zhang, Z. Yu, J. Liu and L. Sun, *ACS Catal.*, 2014, **4**, 2347–2350.

50 Y. Gao, X. Ding, J. Liu, L. Wang, Z. Lu, L. Li and L. Sun, *J. Am. Chem. Soc.*, 2013, **135**, 4219–4222.

51 K. Hanson, M. K. Brennaman, H. Luo, C. R. K. Glasson, J. J. Concepcion, W. Song and T. J. Meyer, *ACS Appl. Mater. Interfaces*, 2012, **4**, 1462–1469.

52 E. Bae, W. Choi, J. Park, H. S. Shin, S. B. Kim and J. S. Lee, *J. Phys. Chem. B*, 2004, **108**, 14093–14101.

53 K. Hanson, M. K. Brennaman, A. Ito, H. Luo, W. Song, K. A. Parker, R. Ghosh, M. R. Norris, C. R. K. Glasson, J. J. Concepcion, R. Lopez and T. J. Meyer, *J. Phys. Chem. C*, 2012, **116**, 14837–14847.

54 K. Hanson, M. D. Losego, B. Kalanyan, G. N. Parsons and T. J. Meyer, *Nano Lett.*, 2013, **13**, 4802–4809.

